CHALMERS
UNIVERSITY OF TECHNOLOGY

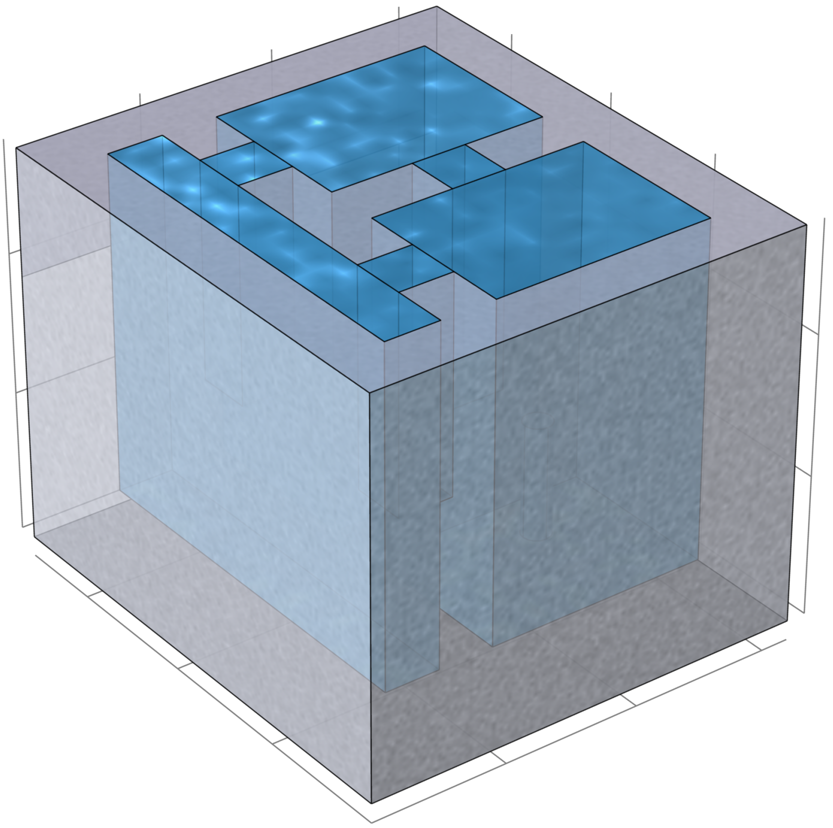

Analysis of Loss of Cooling in Spent Nuclear Fuel Pools

An Improved Analysis of Heat Losses in the Spent Fuel Pools at Units 3 and 4 of Ringhals Nuclear Power Plant

Master's thesis in Master Programme Nuclear Science and Technology

SIMON HOLM
TOM WIKMAN

Department of Physics and Engineering Physics - Nuclear Engineering
CHALMERS UNIVERSITY OF TECHNOLOGY
Gothenburg, Sweden 2019

Master's thesis CTH-NT-340 ISSN 1653-4662

Analysis of Loss of Cooling in Spent Nuclear Fuel Pools

An Improved Analysis of Heat Losses in the Spent Fuel Pools at Units 3 and 4 of Ringhals Nuclear Power Plant

SIMON HOLM
TOM WIKMAN

Department of Physics and Engineering Physics
Division of Nuclear Engineering
Chalmers University of Technology
Gothenburg, Sweden 2019

Analysis of Loss of Cooling in Spent Nuclear Fuel Pools
An Improved Analysis of Heat Losses in the Spent Fuel Pools at Units 3 and 4 of Ringhals Nuclear Power Plant
SIMON HOLM
TOM WIKMAN

Supervisor: Pascal Veber, Ringhals GN-TPP
Examiner: Anders Nordlund, Department of Physics

Master's Thesis CTH-NT-340
Department of Physics and Engineering Physics
Division of Nuclear Engineering
Chalmers University of Technology
SE-412 96 Gothenburg
Telephone +46 31 772 1000

Cover: A simplified geometric representation of the Spent Fuel Pools at Ringhals units 3 and 4.

Typeset in LaTeX
Gothenburg, Sweden 2019

Analysis of Loss of Cooling in Spent Nuclear Fuel Pools
An Improved Analysis of Heat Losses in the Spent Fuel Pools at Units 3 and 4 of Ringhals Nuclear Power Plant
SIMON HOLM
TOM WIKMAN
Department of Physics and Physics Engineering
Chalmers University of Technology

Abstract

This master thesis presents an improved estimate of the course of events in the loss of cooling of the spent fuel pools on Ringhals 3 and 4. Previous analyzes do not take heat losses from the water in the pools into account, leading to large conservatism, especially at lower residual heats as evaporation contributes to the removal of a significant portion of the residual heat. With less conservatism, these results can be used when doing priorities in catastrophic events that causes a loss of cooling in the spent fuel pools.

The analysis in this report also shows that evaporation and a decreasing water level occur before boiling, which in the previous analysis was assumed to occur only when the water reaches 100°C. This result can be used to avoid erroneous assumptions about leaking spent fuel pools that could otherwise be assumed as the cause of a decreasing water level.

In order to obtain these results Comsol Multiphysics has been used. Comsol is a multiphysics software that uses the finite element method to simulate physics. A big part of the work has been spent on exploring the possibilities with Comsol, which was a wish from Ringhals.

Keywords: Ringhals, loss of cooling, spent fuel pool, evaporation, Comsol Multiphysics.

Acknowledgements

We would like to thank all the people that have supported us during this thesis work, without all your help it would not have been possible to realize this work.

We would like to thank Ringhals Nuclear Power Plant for setting up this work and giving us the opportunity to carry it out, with a special thanks to our supervisors, Pascal Veber and Jonas Olandersson.

We would also like to thank our examinator, Anders Nordlund, for your guidance in writing this thesis and planning the presentation of the work.

At last we would also like to thank Comsol Multiphysics for sponsoring this work with their software license and their valuable time in order to support this work.

Simon Holm & Tom Wikman, Gothenburg, June 2019

Contents

List of Figures xi

List of Abbreviations xiii

Nomenclature xv

1 Introduction 1
- 1.1 Aim . . . 1
- 1.2 Scope . . . 2

2 Theory 3
- 2.1 Heat Transfer . . . 3
  - 2.1.1 Conduction . . . 4
  - 2.1.2 Convection . . . 4
    - 2.1.2.1 Forced convection . . . 4
    - 2.1.2.2 Natural Convection . . . 4
  - 2.1.3 Radiation . . . 4
- 2.2 Evaporation . . . 5
- 2.3 Fluid Dynamics . . . 5
  - 2.3.1 Flow conditions . . . 5
- 2.4 Simplified models . . . 5
  - 2.4.1 Natural convection between water and air . . . 6
  - 2.4.2 Evaporation model, Hung . . . 6
  - 2.4.3 Evaporation model, Shah . . . 7

3 Method 9
- 3.1 Selection of Modelling tool . . . 9
  - 3.1.1 Microsoft Excel . . . 9
  - 3.1.2 MATLAB/Simulink . . . 9
  - 3.1.3 Fluent . . . 9
  - 3.1.4 Comsol Multiphysics . . . 10
    - 3.1.4.1 Finite Element Method . . . 10
    - 3.1.4.2 Computational Fluid Dynamics . . . 10
- 3.2 Comsol Multiphysics . . . 10
  - 3.2.1 Geometry . . . 10
  - 3.2.2 Materials . . . 12
  - 3.2.3 Physics Modules . . . 12

3.2.3.1 Heat Transfer Module 12
3.2.3.2 Fluid Flow Module 12
3.2.3.3 Moisture Transport Module 12
3.2.4 Mesh 13
3.2.5 Water Level Change 14
3.3 Simplifications and Assumptions 15
3.3.1 Fuel geometry 15
3.3.2 Heat Radiation 16
3.3.3 Pool lining 16
3.3.4 SFP Building 16
3.3.5 Adjacent buildings 17
3.3.6 Heat distribution 18
3.3.7 Initial temperature and outside temperature 18
3.3.8 Moisture Transport in Air 18
3.3.9 Water Level Change 19

4 Results 21
4.1 Temperatures 21
4.2 Change in Water Level 25
4.3 Sensitivity Studies 29
4.3.1 Relative Humidity 29
4.3.2 Water level 29
4.4 Validation of Evaporation Models 30

5 Conclusion 33

Bibliography 35

List of Figures

2.1 A 2D-sketch of the Spent Fuel Pool (SFP) and the heat transfer modes affecting the analysis. 3

3.1 SFP of one unit with concrete (grey) and water (blue) 11
3.2 Outer walls of fuel building. The areas in red are modelled as thermal insulation to account for adjacent buildings. 11
3.3 Mesh of only water volume 13
3.4 Mesh of SFP and air volume. The mesh has a higher resolution at the water and its boundaries. 14
3.5 SFP water volume. The volumes in red shows the homogeneous heated water volume used in the model to simulate the fuel. 16
3.6 Fuel building with pool, included air volume (shown in grey) and excluded air volume(shown in red). 17
3.7 Outer walls of fuel building. The areas in red are modelled without heat transfer to account for adjacent buildings. 18

4.1 Temperatures for previous and new analysis, 0.5MW 21
4.2 Temperatures for previous and new analysis, 1MW 22
4.3 Temperatures for previous and new analysis, 1.5MW 22
4.4 Temperatures for previous and new analysis, 2MW 23
4.5 Temperatures for previous and new analysis, 3MW 23
4.6 Temperatures for previous and new analysis, 5MW 24
4.7 Temperatures for previous and new analysis, 10MW. Note: The non linear behaviour of the red curve is only due to the data being plotted in full hour steps. 24
4.8 Water levels for previous and new analysis, 0.5MW 25
4.9 Water levels for previous and new analysis, 1MW 26
4.10 Water levels for previous and new analysis, 1.5MW 26
4.11 Water levels for previous and new analysis, 2MW 27
4.12 Water levels for previous and new analysis, 3MW 27
4.13 Water levels for previous and new analysis, 5MW 28
4.14 Water levels for previous and new analysis, 10MW. Note: The non linear behaviour of the red curve is only due to the data being plotted in full hour steps. 28
4.15 Comparisons between analysis' using different relative humidities . . . 29
4.16 Comparisons between analysis' with full water level and 2m lower water level. (Hung model) 30

4.17 Comparison with Fukushima-Daiichi SFP4 equilibrium temperature . 31

List of Abbreviations

CFD Computational Fluid Dynamics. 9, 10, 33

FEA Finite Element Analysis. 10
FEM Finite Element Method. 10
FP Fission Product. 1

NPP Nuclear Power Plant. 1, 2

ODE Ordinary Differential Equation. 14

SFP Spent Fuel Pool. xi, 1–4, 10–14, 16, 21, 29, 30, 33
STF Safety-related Operating Conditions. 18

Nomenclature

β	Thermal expansion coefficient, *dimensionless*
β_m	Analogous thermal expansion coeff. for mass transfer, *dimensionless*
Δh	Water level change, m
ΔV	Volume of evaporated water, m^3
$\Delta \dot{h}$	Water level change rate, m/s
$\dot{m}$	Evaporation mass flow, kg/s
ϵ	Material emissivity, W/m^2
μ	Dynamic viscosity, air at ambient conditions, $Pa \cdot s$
∇T	Temperature gradient, K/m
ω_a	Specific humidity, air at ambient conditions, $kg_{water\,vapor}/kg_{dry\,air}$
ω_s	Specific humidity, air at water surface, $kg_{water\,vapor}/kg_{dry\,air}$
ρ_a	Moist air density at ambient conditions, kg/m^3
ρ_r	Density of dry portion of air at ambient conditions, kg/m^3
ρ_s	Moist air density at water surface, kg/m^3
ρ_w	Density of dry portion of air at water surface, kg/m^3
ρ_{water}	Density of water, kg/m^3
σ	Stefan-Boltzmann constant, $W/m^2, K^4$
A_s	Water surface area, m^2
C_p	Heat capacity of moist air at ambient conditions, $J/kg, K$
C_s	Black body radiation, $W/m^2, T^4$
D	Thermal diffusivity, m^2/s
E	Evaporation rate, $kg/m^2, s$
g	Gravitational constant, m/s^2
Gr	Grashof number, *dimensionless*
Gr_m	Analogous Grashof number for mass transfer, *dimensionless*
h_{fg}	Latent heat of vaporization, J/kg
k	Thermal conductivity, $W/m, K$
L	Characteristic length, m
m	Evaporated mass, kg
Nu	Nusselt number, *dimensionless*
Nu_m	Analogous Nusselt number for mass transfer, *dimensionless*
p_a	Partial pressure of water vapor in air at ambient conditions, Pa
p_s	Partial pressure of water vapor in air at water surface, Pa
Q_c	Heat flux due to convection, W
Q_e	Heat flux due to evaporation, W
Ra	Rayleigh number, *dimensionless*
Ra_m	Analogous Rayleigh number for mass transfer, *dimensionless*

Sc	Schmidt number, *dimensionless*
T_a	Average air temperature, K
T_w	Average water surface temperature, K
v	Kinematic viscosity, m^2/s
q	Heat flux density, $W/m^2, K$

1 Introduction

In a Nuclear Power Plant (NPP), Spent Fuel Pools (SFPs) are used to store spent nuclear fuel, as well as the fuel of the core during refuelling and maintenance outages. This fuel is highly radioactive and the decay of radioactive isotopes, mainly Fission Products (FPs), generates heat that needs to be cooled off. The main objectives of the SFPs are to cool the fuel and provide a sufficient radiation shielding.

In the case of a loss of main and backup power, the cooling system cannot remove the decay heat of the nuclear fuel, and the water temperature will rise. This may lead to boiling of the water, which will in turn lead to a decline in water level, reducing the radiation shielding. If the fuel is uncovered, the ability to remove heat from the fuel is almost completely removed, leading to significant fuel damage and release of FPs.

The current analysis of loss of SFP cooling is done in a very conservative manner. This analysis does not take into account any heat losses from the water in the SFP and assumes a uniform heating of the water to the point of boiling. At the boiling point it is assumed in the old model that all the decay heat causes evaporation of the water, resulting in a declining water level.

Experience from the Fukushima-Daiichi nuclear disaster shows that at lower values for the decay heat the heat losses from the water can be a non negligible part of the decay heat, and even that the water temperature can reach equilibrium temperatures before the boiling point. [11]

Not accounting for evaporation before boiling is a non-conservative assumption with respect to water level and may also cause false assumptions of leakage from the pool if a declining water level is recorded at temperatures below the boiling point.

1.1 Aim

The aim of this thesis is to obtain an improved estimation of the time dependence of the water level and the temperature in the SFP. The water level in the SFP is the main point of interest, since without a sufficient amount of water the fuel cannot be cooled and the surroundings is not shielded from its radiation. The reason for the loss of water is evaporation, which is highly dependent on the temperature in the water and its surrounding air. The temperature in the pool is also important for the work environment in the fuel building as well as safety assessments in regards to the structural integrity of the concrete in the SFP.

This can serve to further the understanding of the behaviour of the SFP during an event that causes loss of cooling, leading to safer operation and better safety analyzes of the NPP. Removing over-conservatism in the safety analysis can also serve as basis to making better priorities during possibly catastrophic events.

Apart from the analysis this thesis aims to evaluate how suitable the software Comsol Multiphysics is for use in this types of analyzes. Comsol is currently not used at Ringhals but it might be of interest if this thesis work proves successful in performing this type of analysis using Comsol.

1.2 Scope

The thesis work will treat the spent nuclear fuel pools at Ringhals units 3 and 4. These being twin reactors, they will for the scope of this work be treated as equal and no separate investigations between the two units will be carried out. The entire analysis is in regard to a single unit and the results are equally applicable to either of the units.

The thesis will only consider the fuel building, meaning that no modelling of the surroundings will be done. Proper boundary conditions will be set at the edges of the building in order to get a model that is as correct as possible while still ensuring conservatism.

The work will only consider the time dependence of the SFPs to the point of boiling. If the water during a catastrophic event reaches boiling temperatures, there is little use in having a less conservative analysis since cooling of the SFPs will be a top priority alongside cooling the core.

2

Theory

In order to get a better estimate of heat losses from SFPs, the physics that are related to the losses needs to be modelled. These are illustrated in Figure 2.1 and will be further described in section 2.1, Heat Transfer.

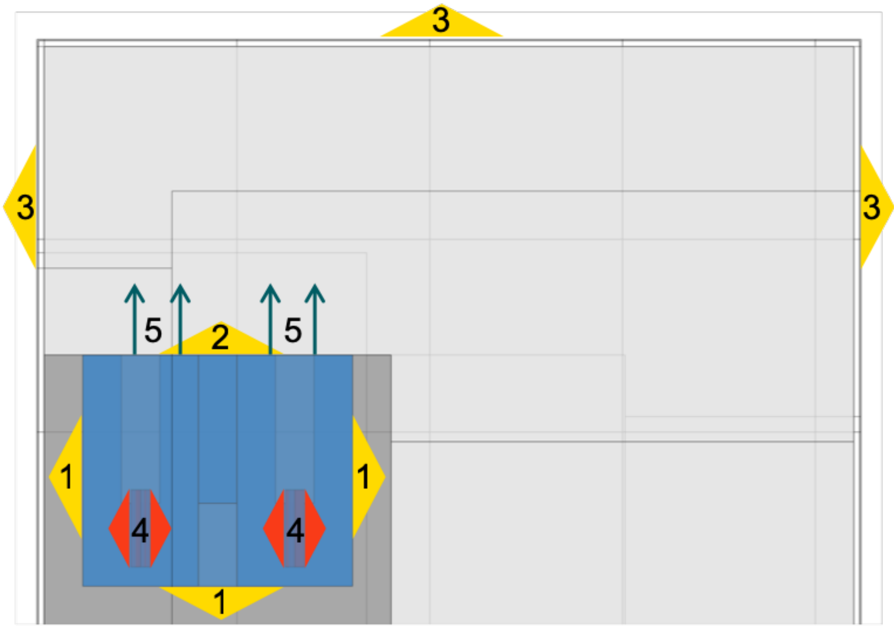

Figure 2.1: A 2D-sketch of the SFP and the heat transfer modes affecting the analysis.

1. Heat transfer to concrete
2. Heat transfer to air
3. Heat losses through outer walls
4. Heat radiation from the fuel
5. Evaporation

2.1 Heat Transfer

The main phenomenon to study in order to get an understanding of the temperature behaviour in the SFPs is the transfer of heat, since heat is produced in the spent fuel and transferred to the rest of the system. In this section the heat transfer modes that has an impact on the system in this analysis is described.

2.1.1 Conduction

Heat is transferred by conduction in solids and static fluids. The driving force is the spatial difference in temperature, and the heat transfer is modelled using Fourier's law [6] that states that the heat flux is proportional to the negative temperature gradient:

$$q = -k \cdot \nabla T \quad [\frac{W}{m^2}] \tag{2.1}$$

2.1.2 Convection

Heat is transferred by convection when one or more of the domains is a moving fluid. Fourier's law still applies, but the temperature gradient is affected by the motion of the fluid.

2.1.2.1 Forced convection

Motion in a fluid that is driven by an external force is called forced convection. In the SFP there is forced convection in the water due to the pumps of the cooling system and in fuel building there is forced convection in the air due to ventilation. Since the premise for the analysis is a loss of cooling, the forced convection in the SFP ceases. The cause of the loss of cooling will also almost certainly also cause a power loss to the ventilation, meaning that no forced ventilation will be included in the analysis.

2.1.2.2 Natural Convection

Materials change their density with a changing temperature. When a density gradient occurs in a fluid, a flow can occur due to gravitational forces. When heat is transferred this way it is called natural convection. [6]

2.1.3 Radiation

Any solid or liquid surface emits heat radiation. Heat transfer by radiation is a transfer of heat energy by electromagnetic radiation, and thus does not require a medium to be transported in.
The amount of heat transfer by radiation is defined by:

$$q = \epsilon \cdot C_s \cdot (\frac{T}{100})^4 \quad [\frac{W}{m^2}] \tag{2.2}$$

where C_s is the *radiation of black bodies*:

$$C_s = 10^8 \cdot \sigma = 5.67 \quad [\frac{W}{m^2 \cdot T^4}] \tag{2.3}$$

and ϵ is the material emissivity [6]

2.2 Evaporation

When a wet surface is in contact with air that is not saturated with water vapour evaporation occurs. In order for water to evaporate it has to receive an amount of energy equal to its latent heat. Therefore, when water evaporates from a surface it causes a removal of heat from that surface [5]:

$$Q_e = h_{fg} \cdot \dot{m} \tag{2.4}$$

When water evaporates it raises the concentration of water vapour in the air in the immediate vicinity of the water surface. The moisture then transfers to the rest of the air volume either by convection or by diffusion. Diffusion is a very slow process in comparison to the spread of water vapour by convection, therefore air movement is necessary for evaporation to have a significant effect. [7]

2.3 Fluid Dynamics

Fluid dynamics, which is a subset of fluid mechanics, physically describes the flow of fluids. The flow condition in a fluid is important in fluid-dynamics problems since it subsequently affects heat- and mass transfer in the system [1]. Therefore, the flow conditions governing the problem will be further described.

2.3.1 Flow conditions

The fluid motion of natural convection is complex which makes it hard to obtain simple analytical relations for heat transfer by solving the governing equations of motion and energy. The flow condition in natural convection is denoted by the Grashof number, which is the ratio of the buoyancy force to the viscous force acting on the fluid. It is the analogous form of the commonly known Reynolds number, which is used to denote the flow condition of forced convection. A lower Grashof number denotes a laminar flow while a higher Grashof number denotes a turbulent flow.[4]

2.4 Simplified models

In some cases simplified models are needed for physical phenomena in order to reduce computational complexity. A simplified model for heat transfer by convection at the water surface, developed by Hung, is used in this analysis. Two simplified models for evaporation, Hung and Shah, are also described in this section. In the continuation these two models are used for evaporation due to their similar behaviour even though they are different in their way of determining evaporation. No evaluation is being made in regards to which model is the most correct.

2.4.1 Natural convection between water and air

Hung [7] proposes a simplified model for heat transferred between the water surface and the air via natural convection that can be expressed as:

$$Q_c = Nu \cdot \frac{kA}{L} \cdot (T_s - T_a) \tag{2.5}$$

with the Nusselt number calculated as[8]:

$$Nu = 0.54Ra^{1/4} \quad 10^4 \leq Ra \leq 10^7 \tag{2.6}$$

$$Nu = 0.15Ra^{1/3} \quad 10^7 \leq Ra \leq 10^{11} \tag{2.7}$$

with the Rayleigh number calculated as[4]:

$$Ra = Gr \cdot Pr \tag{2.8}$$

and with Grashof and Prandtl defined as[4]:

$$Gr = \frac{g\beta(T_s - T_a)L^3}{v^2} \tag{2.9}$$

$$Pr = \frac{C_p\mu}{k} \tag{2.10}$$

2.4.2 Evaporation model, Hung

Hung [7] proposes an analogous model for heat removed by evaporation due to similarity between heat and mass transfer:

$$Q_e = Nu_m \cdot h_{fg} \cdot D \cdot (\rho_a - \rho_s) \cdot A_s/L \tag{2.11}$$

with the analogous Nusselt number(also known as the Sherwood number) calculated as[8]:

$$Nu_m = 0.54Ra_m^{1/4} \quad 10^4 \leq Ra_m \leq 10^7 \tag{2.12}$$

$$Nu_m = 0.15Ra_m^{1/3} \quad 10^7 \leq Ra_m \leq 10^{11} \tag{2.13}$$

with the analogous Rayleigh number, Ra_m, calculated by substituting the Prandtl number for the Schmidt number:

$$Ra_m = (Gr + Gr_m) \cdot Sc \tag{2.14}$$

with the analogous Grashof number,Gr_m and Schmidt number defined as[11]:

$$Gr_m = \frac{g\beta_m(\omega_s - \omega_a)L^3}{v^2} \tag{2.15}$$

$$Sc = \frac{v}{D} \tag{2.16}$$

2.4.3 Evaporation model, Shah

For evaporation in case of natural convection, Shah uses the analogy between heat- and mass transfer. The water surface is modelled as a heated horizontal plate facing upwards, giving the following equation for evaporation rate [10]:

$$E = \frac{35}{3600} \cdot \rho_w (\rho_r - \rho_w)^{1/3} \cdot (\omega_s - \omega_a) \tag{2.17}$$

In cases where the air density at the water surface is greater than the ambient density, natural convection ceases substantially and air movement needed to remove saturated air from the water surface depends entirely on the air currents caused by other effects in the room [10]. By analyzing empirical data, Shah proposes the following equation:

$$E = \frac{0.00005}{3600} \cdot (p_w - p_r) \tag{2.18}$$

For pools without forced convection in the air, the evaporation rate is calculated as the larger E from equations 2.17 and 2.18 [10].

Combining this with (2.4) gives the following formula for the heat flux due to evaporation according to Shah:

$$Q_e = E \cdot h_{fg} \cdot A_s \tag{2.19}$$

3
Method

In this chapter the methodology of the work is presented. Here the selection process for the calculation tool is presented, the selected tool is described more in depth and then the input for the calculations and custom built models are presented. The chapter ends with descriptions of the simplifications made in order to reduce complexity of the model.

3.1 Selection of Modelling tool

Several options were considered to select modelling tool. Tools that have been considered are Microsoft Excel, MATLAB, Fluent and Comsol Multiphysics.

3.1.1 Microsoft Excel

The previous analysis was carried out using Microsoft Excel. It was suitable for that analysis since its simplifications made it possible to set up single equations for the sought parameters, such as time to a certain temperature or time to reduced shielding. Including the physics described in chapter 2, Theory does not allow for single equations to be set up, therefore the idea of using Excel was disregarded.

3.1.2 MATLAB/Simulink

The second option considered for carrying out the analysis was using MATLAB or Simulink to set up differential equations for the different volumes, their temperatures and the heat transfer between them. This would however only be able to account for uniform heat distribution in each volume and not the flow in the air and water, or any other local effects of the heat transfer.

3.1.3 Fluent

Ansys Fluent is currently used at Ringhals for Computational Fluid Dynamics (CFD). Being a traditional CFD tool it would probably have been suitable for this work. The main reasons it was not chosen was that it would probably have been very computationally expensive, and Ringhals were interested in evaluating a new tool rather than use one of the tools already available.

3.1.4 Comsol Multiphysics

Comsol is a multiphysics software that utilizes the Finite Element Method (FEM), therefore it has the ability to capture local phenomena very well. It also has CFD capabilities, so the flow in the water and air volumes could be modelled. The main feature with Comsol is the multiphysics capabilities. The software includes a lot of modules for different physics, and each of these modules is highly customizable. When physics of different modules are depending on each other they can also be coupled together using multiphysics interfaces.

3.1.4.1 Finite Element Method

The FEM is a method where a system with a problem described by analytical equations is divided into smaller geometries, called finite elements. This way the governing equations are discretized spatially and can then be solved using numerical approximations. The network of finite elements is called a mesh. Using FEM to analyze problems is often referred to as Finite Element Analysis (FEA).

3.1.4.2 Computational Fluid Dynamics

CFD is an approach to numerically solve the equations governing fluid flow in a volume. Using FEM is one way among others to spatially discretize a volume for CFD analysis. The transport equations governing flow, namely the Navier-Stokes equations, can then be solved using numerical methods.

3.2 Comsol Multiphysics

In this section the input data specified in Comsol is described. All of the inputs are in regard to a single unit, and since unit 3 and 4 are considered equal it can apply to either of them.

3.2.1 Geometry

The geometry of the model was built in Comsol based on technical drawings with various simplifications being made in order to reduce complexity. A detailed description of simplifications can be found in section 3.3, Simplifications and Assumptions. Due to the drawings being classified there is no detailed description of the geometry or its dimensions. The SFP consist of two pools, a transport channel and channels between them with surrounding concrete, see Figure 3.1.

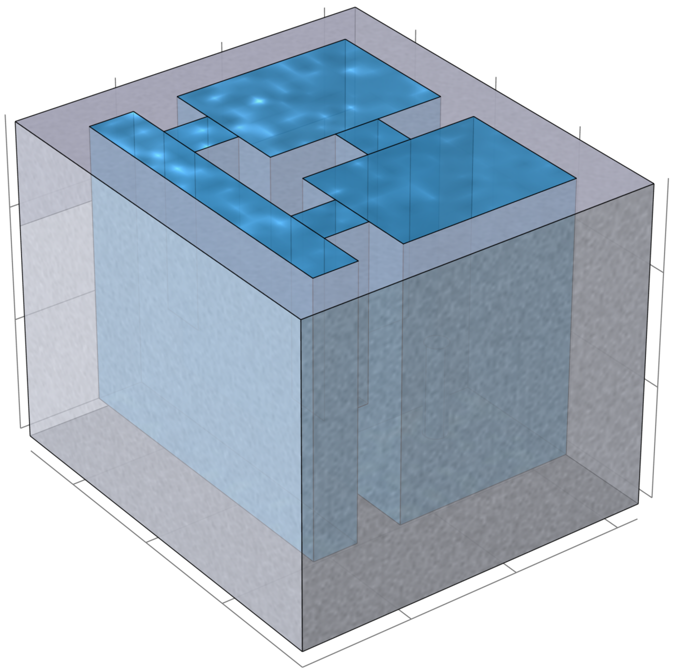

Figure 3.1: SFP of one unit with concrete (grey) and water (blue)

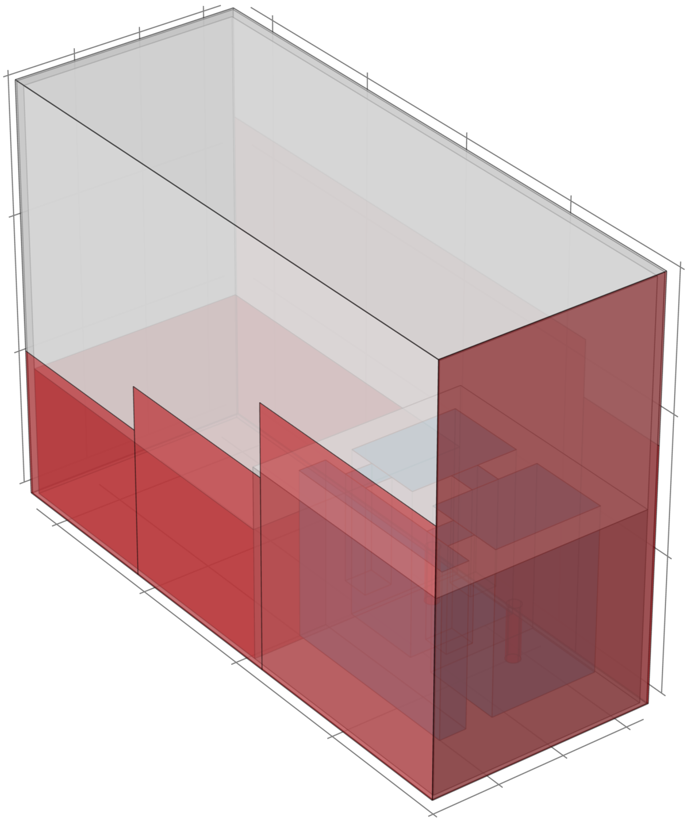

Figure 3.2: Outer walls of fuel building. The areas in red are modelled as thermal insulation to account for adjacent buildings.

The fuel building consists of the SFP and air surrounded by concrete walls, see Figure 3.2

3.2.2 Materials

The materials used in the analysis are water, concrete, air and glass wool. All are available in Comsol's material database, which contains most properties for many materials. Therefore, no calculations on material properties has been made.

3.2.3 Physics Modules

As mentioned in chapter 2, Theory, the different physical phenomena present makes it neccessary to include several models in the analysis in order to get an estimate of the heat losses from the water. The physics modules that was used in the analysis will be further described in this section.

3.2.3.1 Heat Transfer Module

In order to model the heat transport in selected volumes, the heat transfer module was used. The module evaluates the temperature transport in these volumes. However, in order to get a good estimation of the heat transport boundary conditions needed to be applied in the module. Boundary conditions that were applied were heat flux on boundaries, temperatures on boundaries and thermal insulation on boundaries (meaning that there is no heat transfer on these boundaries). A generation of heat was also applied, which in this analysis is the residual heat from the fuel.

3.2.3.2 Fluid Flow Module

The fluid flow was applied to the water and the air volumes through the fluid flow module. As mentioned in subsubsection 2.1.2.2, Natural Convection, the flow in this analysis is natural convection, which is driven by density gradients. The density depends on the temperature which depends on the heat transfer and the heat transfer in its turn depends on the fluid flow. Because these physics are strongly dependent on each other, they were coupled through Comsol's multiphysics interface.

3.2.3.3 Moisture Transport Module

The moisture transport module was also used in order to model evaporation from the water surface and condensation on the outer walls of the building. However, when the module was coupled together with the heat transfer- and fluid flow module through the multiphysics interface it did not converge. Even with help from Comsol's support and development department, no success was reached using the module, and it was therefore not used for the results of the work. Instead the two empirically developed models for evaporation, Hung and Shah, described in section 2.2, Evaporation were implemented as heat removed from the water surface in the heat transfer module, with Q_e evenly distributed across the surface.

3.2.4 Mesh

The mesh in the model was automatically created by Comsol, but its quality was set manually. The quality of the mesh impacts the accuracy of the model, a finer mesh is more accurate, but the computational power required increases as there are more elements. When manually defining the quality of the mesh different volumes and surfaces can be set to have different levels of quality. In this model the mesh was set as finer at the water and its boundaries compared to the rest of the geometries, since the water was the main focus in the study.

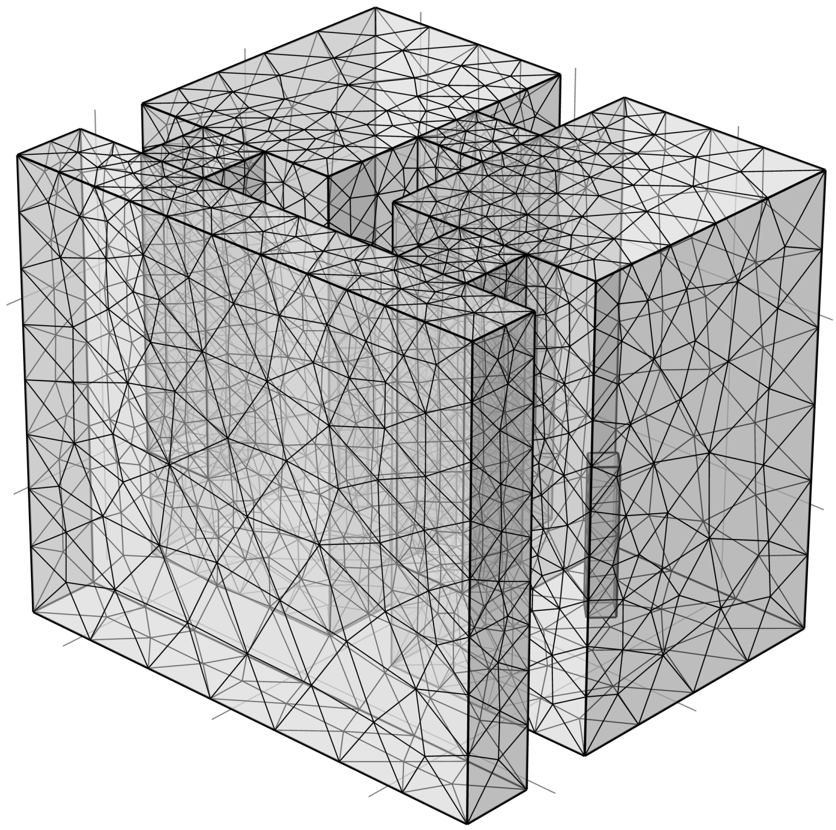

Figure 3.3: Mesh of only water volume

The overall quality of the mesh was determined by a trial-and-error approach, starting with a very coarse mesh, increasing the quality until consistent results were obtained. No convergence studies of the mesh were performed, instead the model was verified by comparing it to measured data from the Fukushima-Daiichi SFP 4. The comparison is further described in section 4.4, Validation of Evaporation Models.

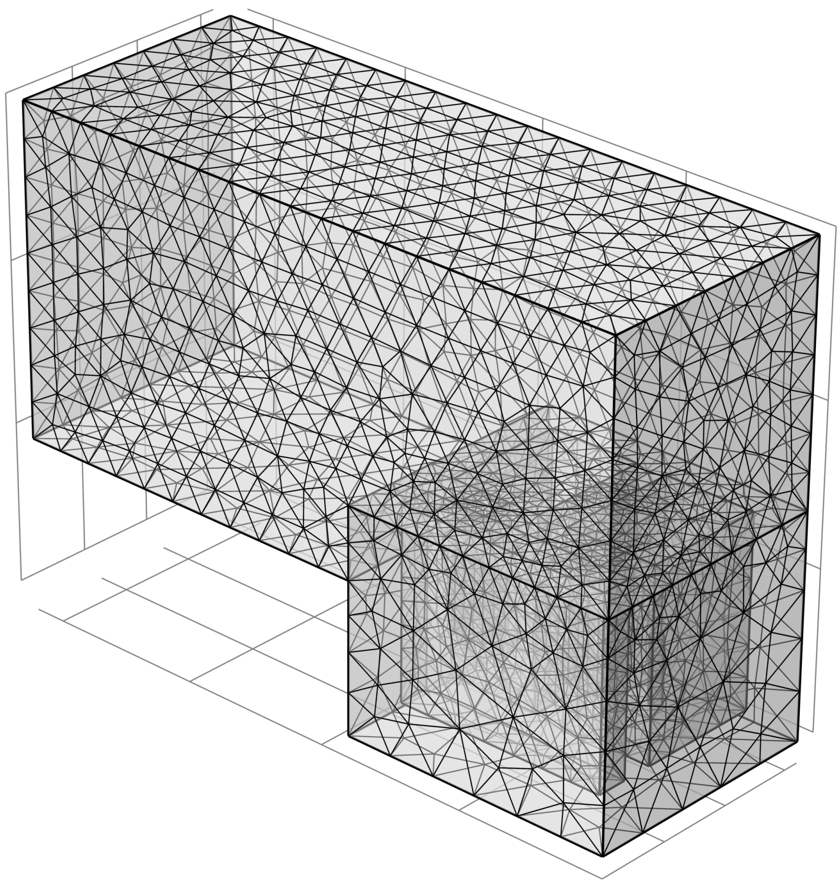

Figure 3.4: Mesh of SFP and air volume. The mesh has a higher resolution at the water and its boundaries.

The mesh of the model contains about 50 000 elements, see Figure 3.4.

3.2.5 Water Level Change

As evaporation of water occurs, the water level in the pools will also change. The change in water level due to evaporation can be described as:

Hung:

$$\Delta h = -\frac{\Delta V}{A_s} = -\frac{m}{\rho_{water} \cdot A_s} = -\frac{1}{\rho_{water} \cdot A_s} \cdot \int_0^t \frac{Q_e}{h_{fg}} dt \tag{3.1}$$

Shah:

$$\Delta h = -\frac{\Delta V}{A_s} = -\frac{m}{\rho_{water} \cdot A_s} = -\frac{1}{\rho_{water} \cdot A_s} \cdot \int_0^t E dt \tag{3.2}$$

Modelling the water level change was done by using a Comsol module for global Ordinary Differential Equations (ODEs). This was done by using the equations (3.1) and (3.2) in their differential form:

Hung:

$$\Delta\dot{h} = -\frac{Q_e}{h_{fg} \cdot \rho_{water} \cdot A_s} \qquad \Delta h(0) = 0 \tag{3.3}$$

Shah:

$$\Delta\dot{h} = -\frac{E}{\rho_{water} \cdot A_s} \qquad \Delta h(0) = 0 \tag{3.4}$$

This change in water level was however not implemented geometrically during the simulations. See subsection 3.3.9, Water Level Change

3.3 Simplifications and Assumptions

In order to obtain a model with reasonable complexity some simplifications were made. These are described here and their impact on uncertainty or conservatism are discussed.

3.3.1 Fuel geometry

The fuel has a geometry consisting of very small details, mainly a lot of small rods with a diameter in the order of roughly 10 mm. Each fuel assembly has hundreds of fuel rods, and there can be hundreds of fuel assemblies in the pool at the same time. A model containing all these details would be virtually impossible to run. The heat output from the fuel was therefore modelled as a separate region in the water volume with the residual heat added, see Figure 3.5

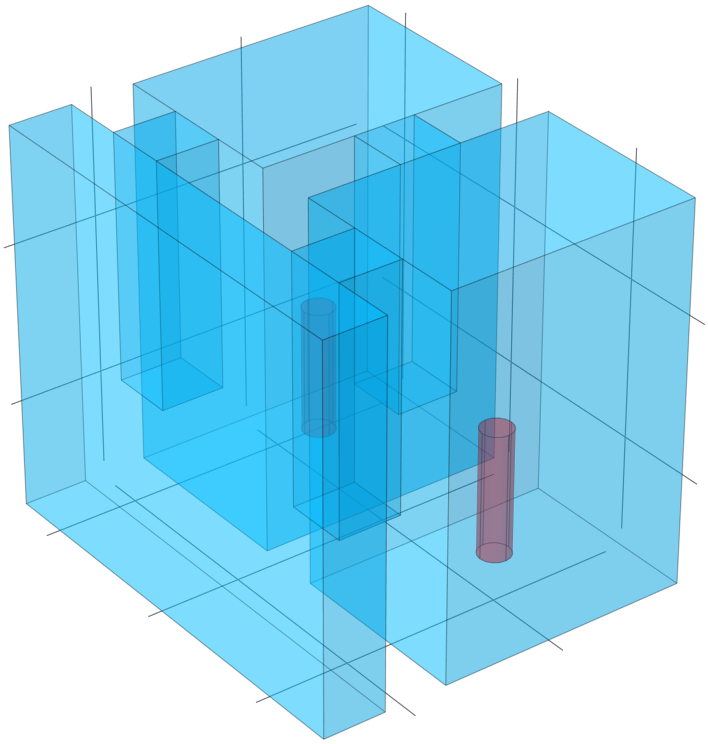

Figure 3.5: SFP water volume. The volumes in red shows the homogeneous heated water volume used in the model to simulate the fuel.

3.3.2 Heat Radiation

Since the fuel geometry was modelled as part of the water volume, the outside temperature of the fuel assembly could not be modelled. This means that the heat radiation from the fuel could not be modelled either. However, the assumption is still considered conservative since all the residual heat from the fuel assembly is spread to the water with no accumulation of heat in the fuel elements.

3.3.3 Pool lining

The pool is lined with plates of stainless steel with vertical channels built into them. In order to reduce the complexity of the model these features were removed, due to their thickness being in the order of a couple of millimeters. Because of the thin thickness of the plates and the fact that steel has much better thermal conductivity than both water and concrete, the impact on the heat transfer is negligible.

3.3.4 SFP Building

In order to further reduce complexity of the computational model, all objects except the pools and the building walls were excluded. This might have a non-conservative impact on the pool temperature since the total heat capacity of the air volume might be overestimated. A part of the air volume was therefore removed in order to counteract any non-conservatism. The volume that has been removed is shown in Figure 3.6.

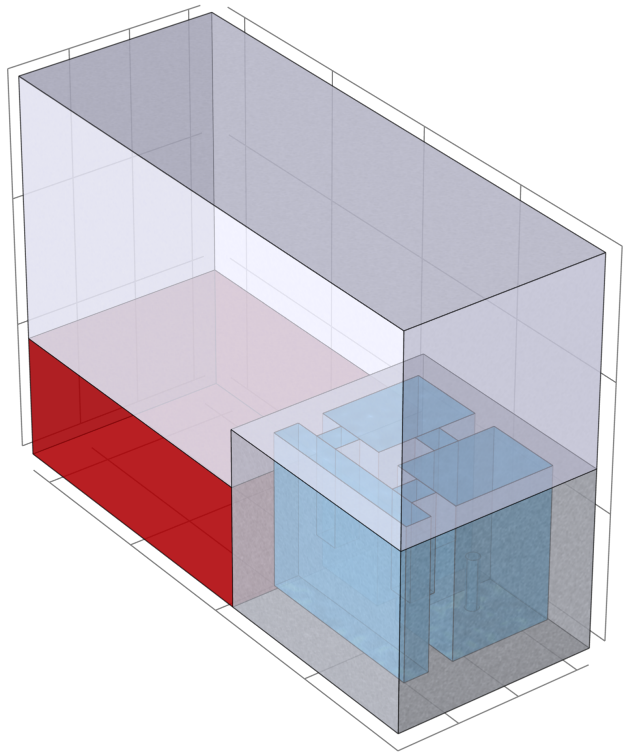

Figure 3.6: Fuel building with pool, included air volume (shown in grey) and excluded air volume(shown in red).

3.3.5 Adjacent buildings

The scope of the work is limited to the fuel building, but surfaces to adjacent buildings was still taken into account, see Figure 3.7. At these surfaces no heat transfer was modelled, since the modelling of the temperature from these becomes would be too extensive for the scope of the work. However, this assumption is considered conservative because heat losses at these surfaces were not included.

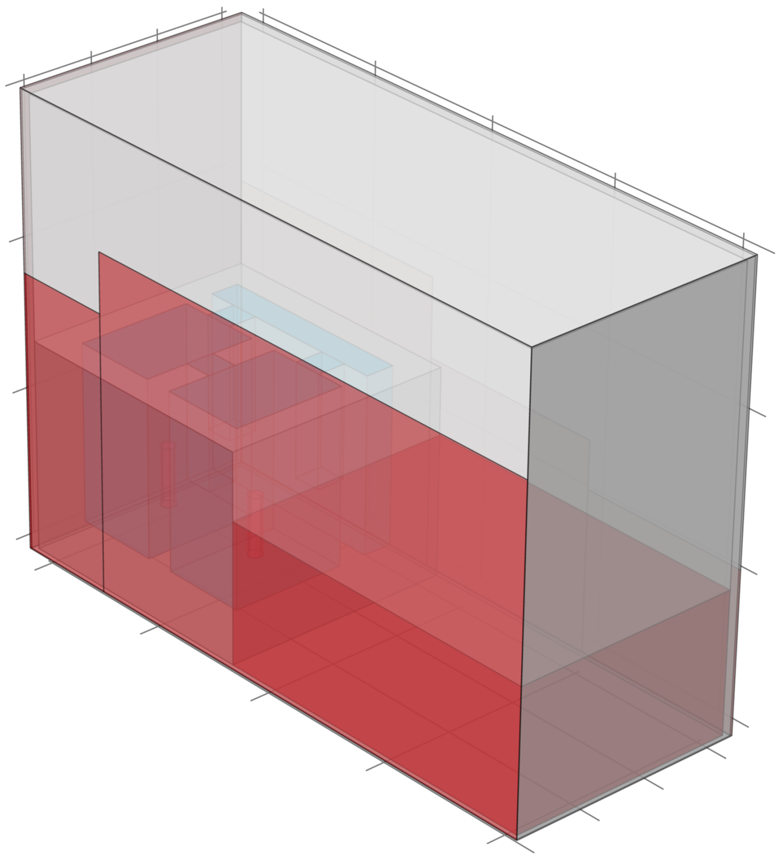

Figure 3.7: Outer walls of fuel building. The areas in red are modelled without heat transfer to account for adjacent buildings.

3.3.6 Heat distribution

The heat from the fuel assemblies should be evenly distributed between the two pools according to Safety-related Operating Conditions (STF). Therefore, an even distribution of the residual heat has been assumed. The residual heat is also assumed to be constant, since the decrease in residual heat during the time frame of the simulations is negligible.

3.3.7 Initial temperature and outside temperature

The initial temperature for the entire model has been set to 20°C. Even the outside temperature has been set to 20°C. Any non-conservatism at a reasonable outside temperature higher than 20°C is is deemed less than the effect of that the surfaces of the adjacent buildings are removed.

3.3.8 Moisture Transport in Air

Since moisture transport is very computationally demanding and no applicable models regarding condensation have been found, condensation have not been modelled.

This also means that relative humidity cannot properly modelled, and has therefore been assumed constant. Due to this assumption being made, a sensitivity study has been made on relative humidity and is further described in section 4.3, Sensitivity Studies.

3.3.9 Water Level Change

A change in water level has not been modelled in the geometry during the simulations. Although, the difference in water level was calculated with the expressions in subsection 3.2.5, Water Level Change. Since an interface that allows the geometry to change over time was not studied in Comsol, and the modules used does not contain such feature, it is not included in the model.

To determine the impact of this simplification a sensitivity study was performed in regards to water level, see subsection 4.3.2, Water level.

4
Results

In this chapter the results obtained from the simulations are presented. The results are shown as temperatures, change in water level, sensitivity studies and validation of evaporation models.

4.1 Temperatures

Graphs for all results concerning temperature change over time are shown in Figure 4.1-4.7. The figures contain temperature curves from simulations within residual heat of 0.5-10 MW. The results indicate that the losses from the water in the SFP are much more significant at lower residual heats than at higher residual heats, leading to a more significant difference in the temperature behaviour between the previous analysis and the current. The lower values (0.5-1.5 MW) for the residual heat correspond to values that are typically in the SFP between outages. During outages the residual heat can reach even higher values than 10 MW, but since the difference between the current and the previous analysis decreases with increased residual heat those values are not of interest in this study.

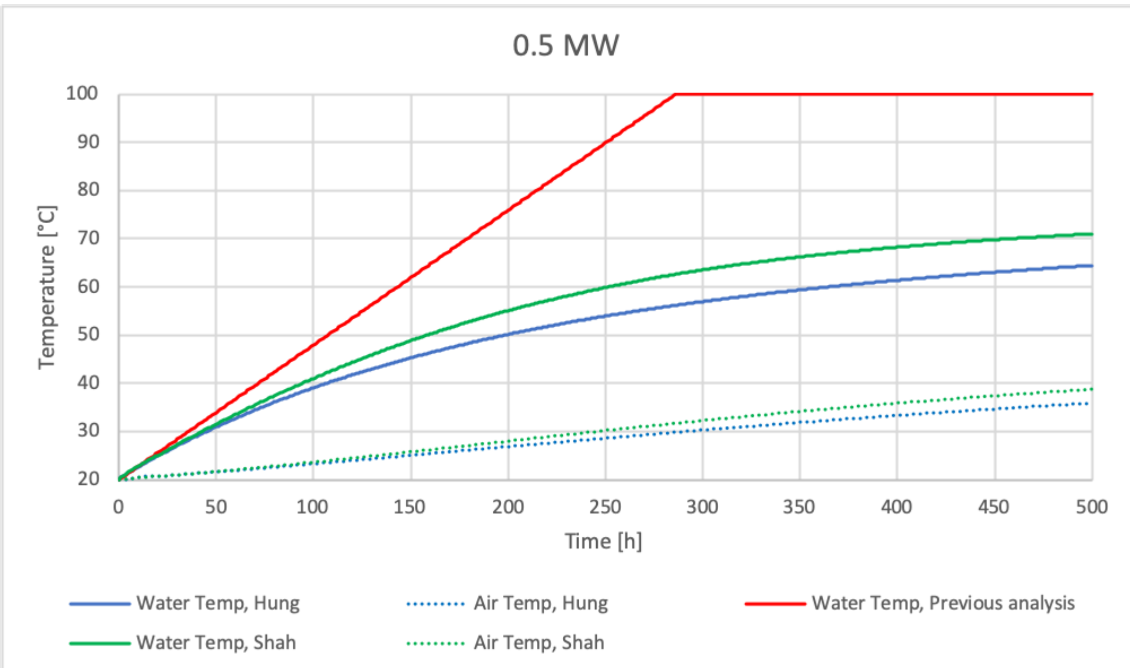

Figure 4.1: Temperatures for previous and new analysis, 0.5MW

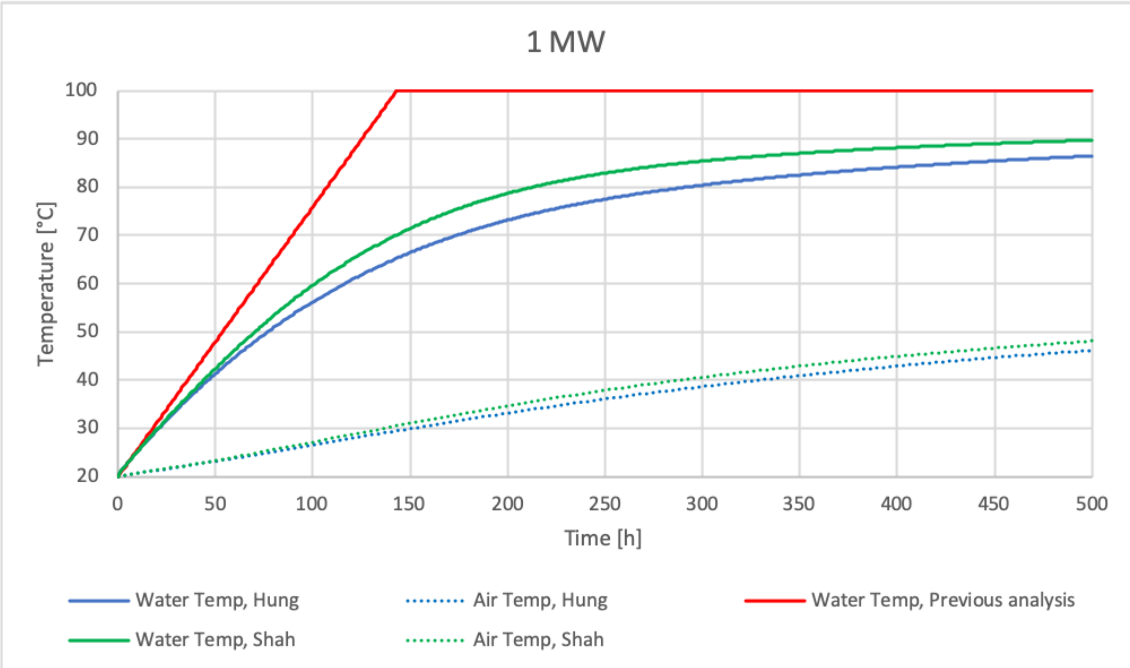

Figure 4.2: Temperatures for previous and new analysis, 1MW

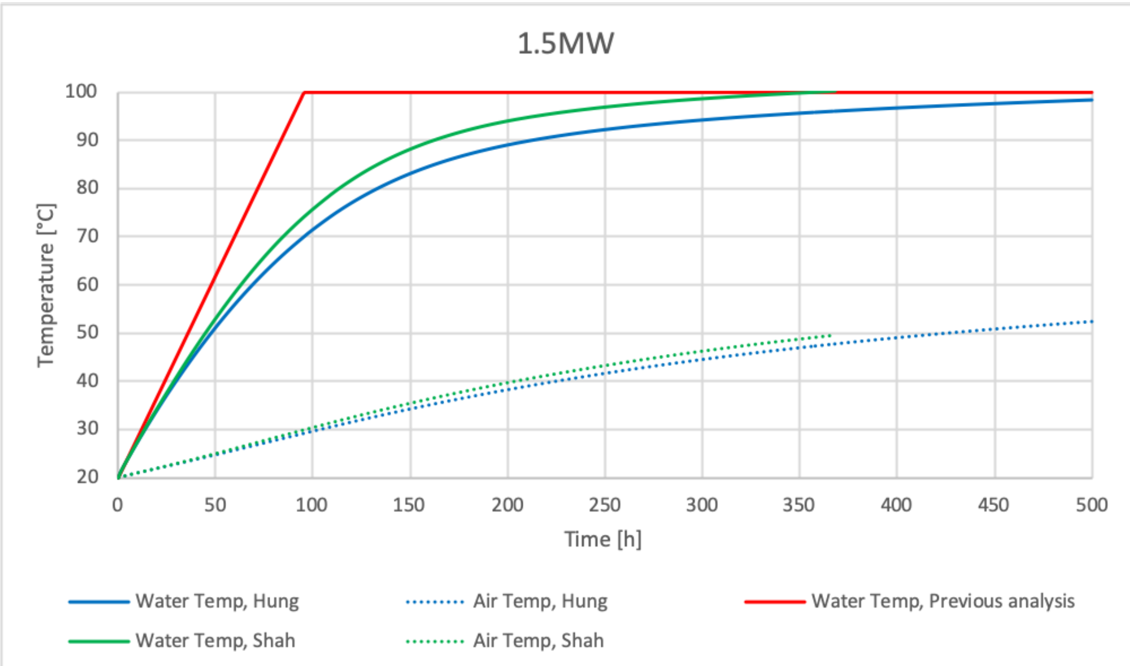

Figure 4.3: Temperatures for previous and new analysis, 1.5MW

At 1.5 MW the effect of the different heat losses can be seen clearly. At lower temperatures, the temperature in the water shows almost the same behaviour as the previous analysis. This is due to the convective heat transfer being dominant, but small in comparison to the residual heat. However, as temperature in the water increases, the evaporation rate increases and therefore the heating of the water decreases and the temperature almost reaches an equilibrium temperature. This is due to the total heat losses reaching the level of the residual heat.

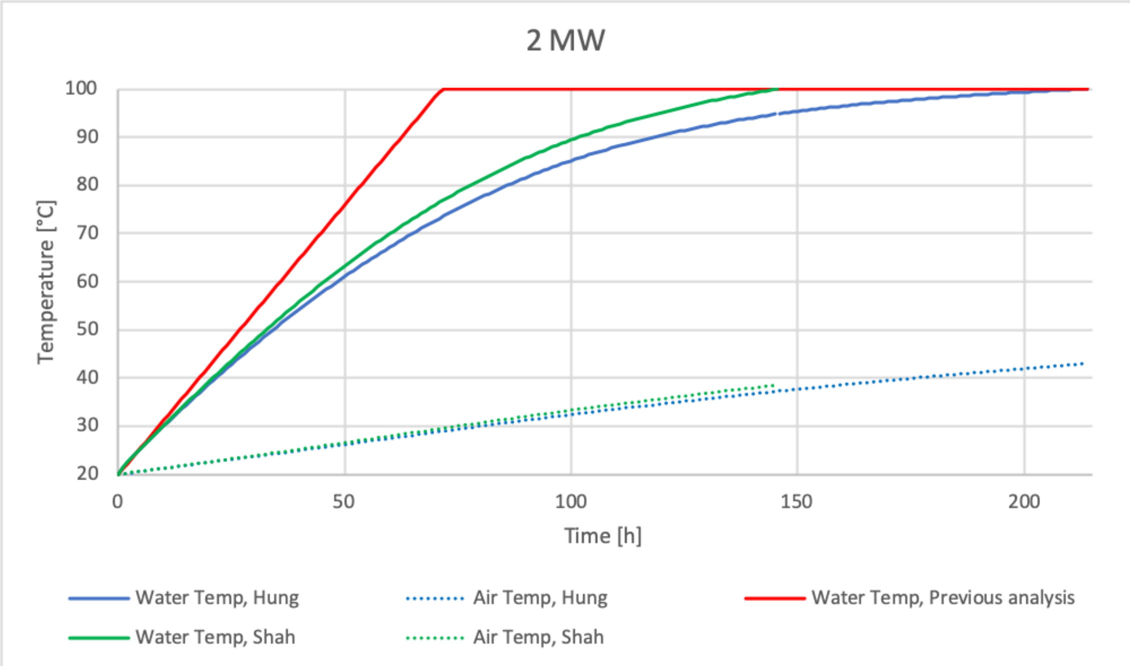

Figure 4.4: Temperatures for previous and new analysis, 2MW

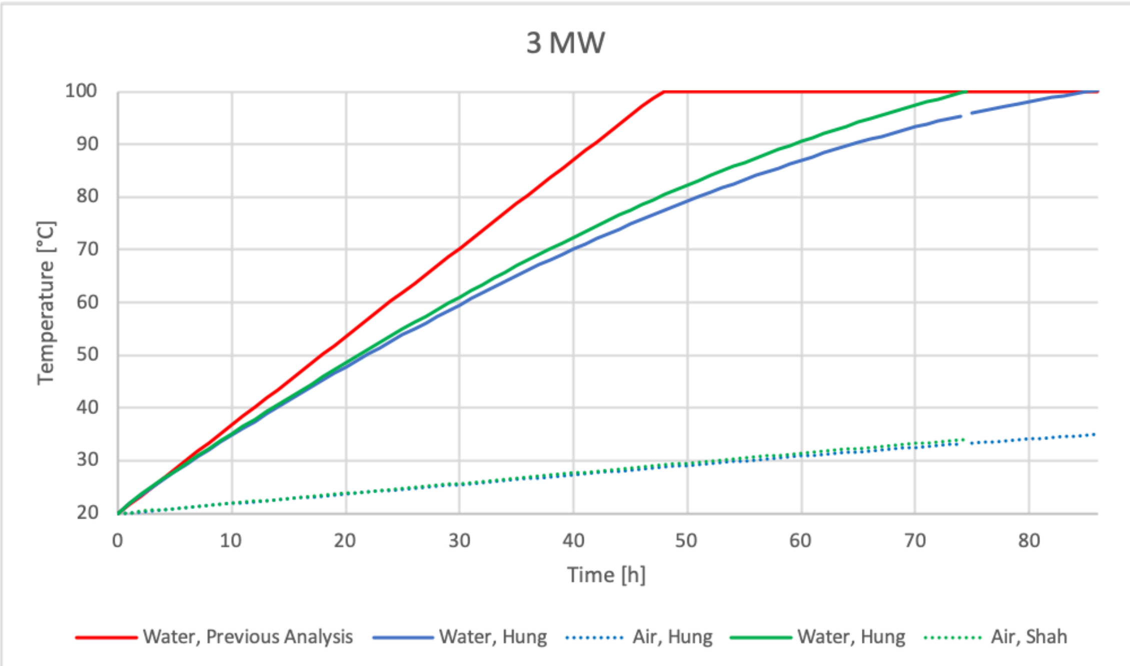

Figure 4.5: Temperatures for previous and new analysis, 3MW

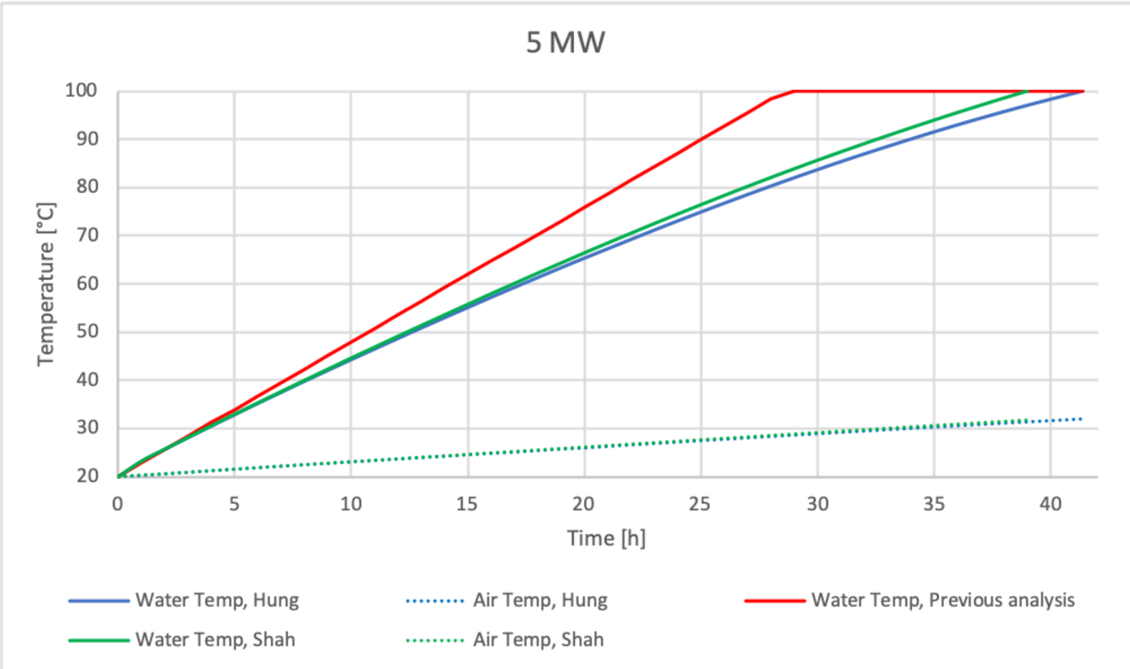

Figure 4.6: Temperatures for previous and new analysis, 5MW

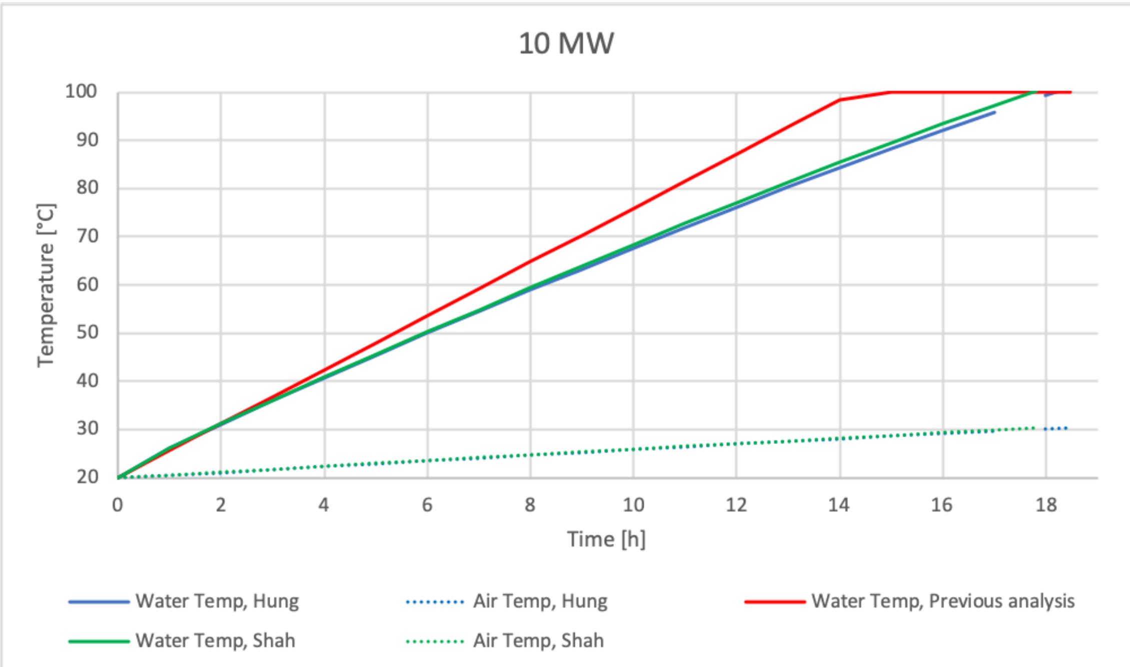

Figure 4.7: Temperatures for previous and new analysis, 10MW. Note: The non linear behaviour of the red curve is only due to the data being plotted in full hour steps.

At higher values for the residual heat it can be seen that the difference between the current and previous analysis becomes much smaller than for lower residual heat. The heat losses does not increase much when the residual heat is increased, therefore the heat losses are smaller compared to the residual heat and therefore less significant.

4.2 Change in Water Level

Graphs for all results concerning water level change over time are shown in Figure 4.8-4.14. The figures contain change in water level from simulations with residual heats of 0.5-10 MW. The results clearly show that the previous analysis´ disregard of evaporation before boiling not is conservative in regard to water level. For 1.0 MW to 2.0 MW it can be seen that as the water level change rate approaches a maximum value, where the total heat loss is in equilibrium with the residual heat, the slope of the water level change curve almost reaches that of the previous analysis. This is because the evaporation is the dominant heat loss, and it does therefore not differ much from the evaporation rate in the previous analysis.

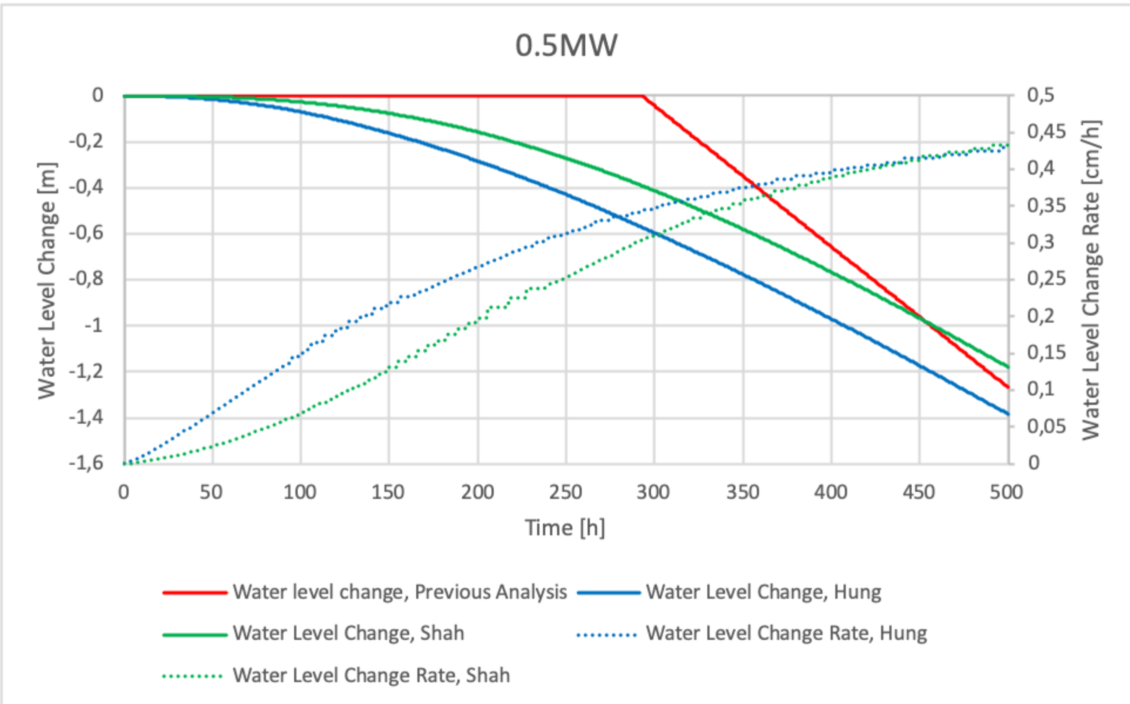

Figure 4.8: Water levels for previous and new analysis, 0.5MW

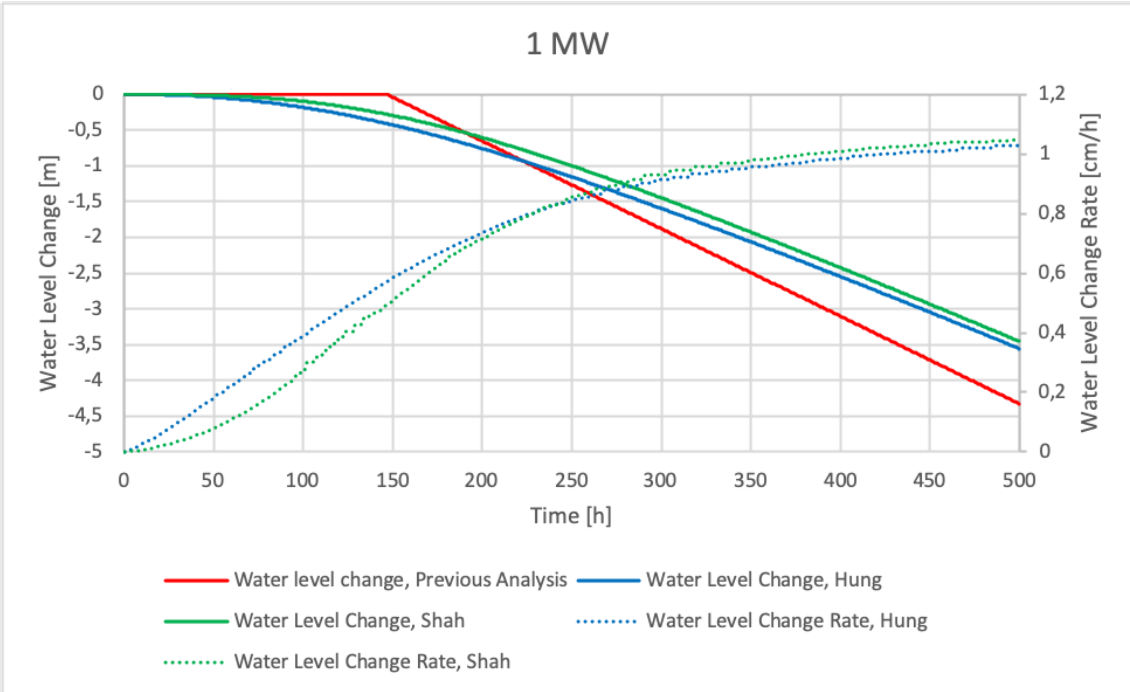

Figure 4.9: Water levels for previous and new analysis, 1MW

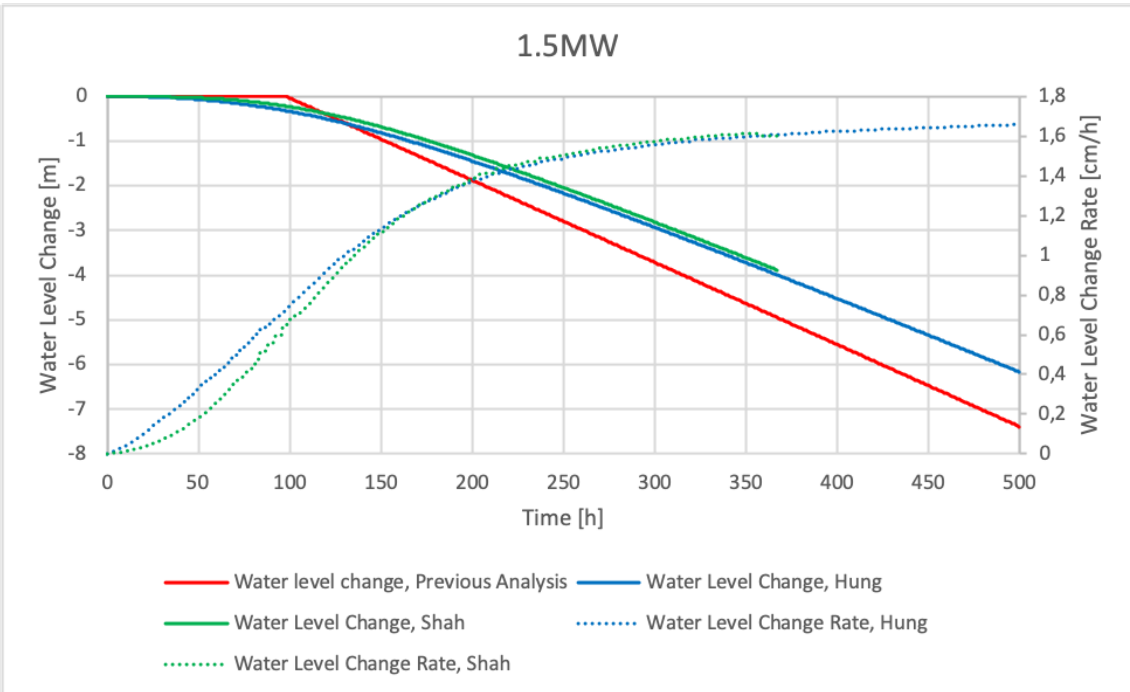

Figure 4.10: Water levels for previous and new analysis, 1.5MW

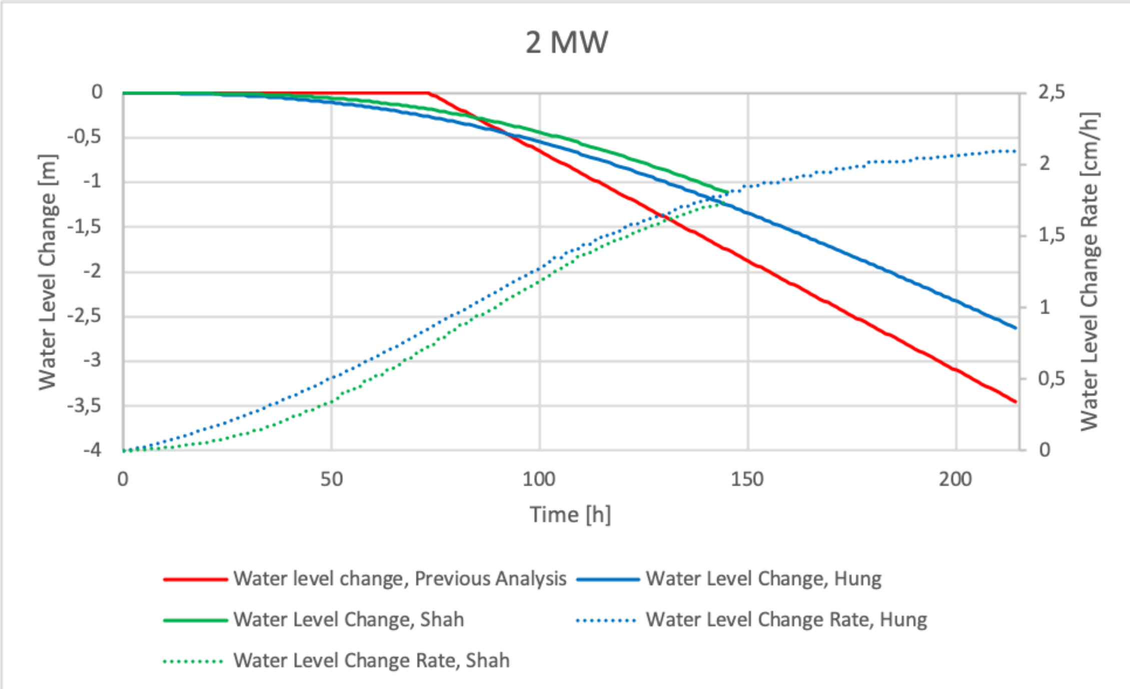

Figure 4.11: Water levels for previous and new analysis, 2MW

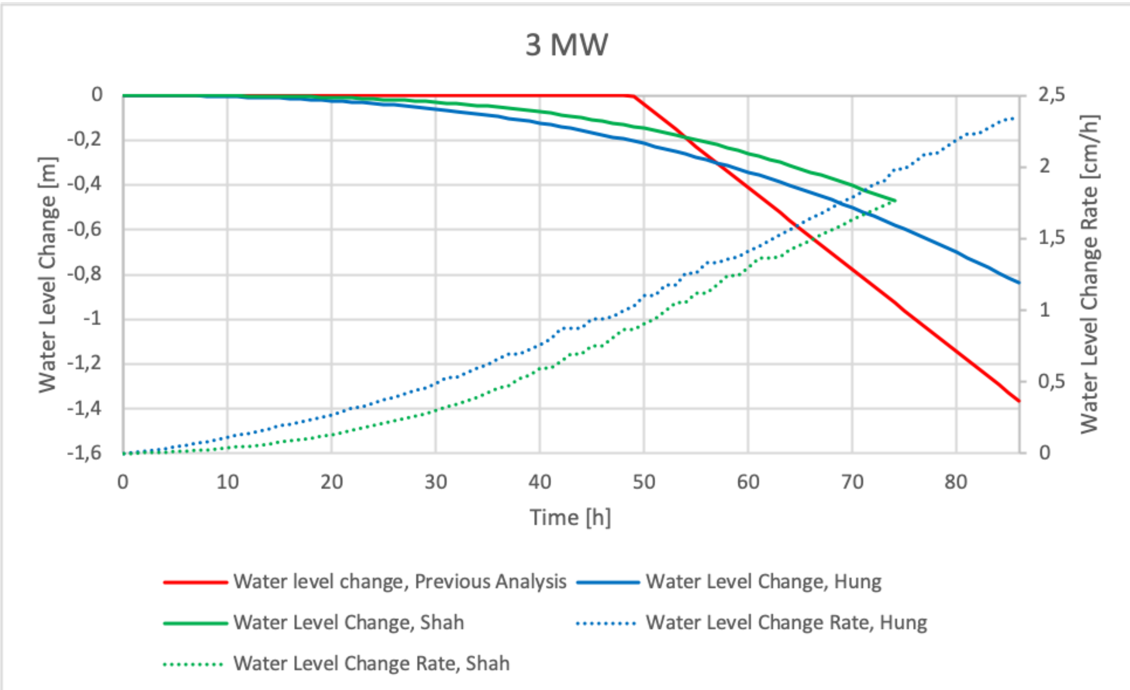

Figure 4.12: Water levels for previous and new analysis, 3MW

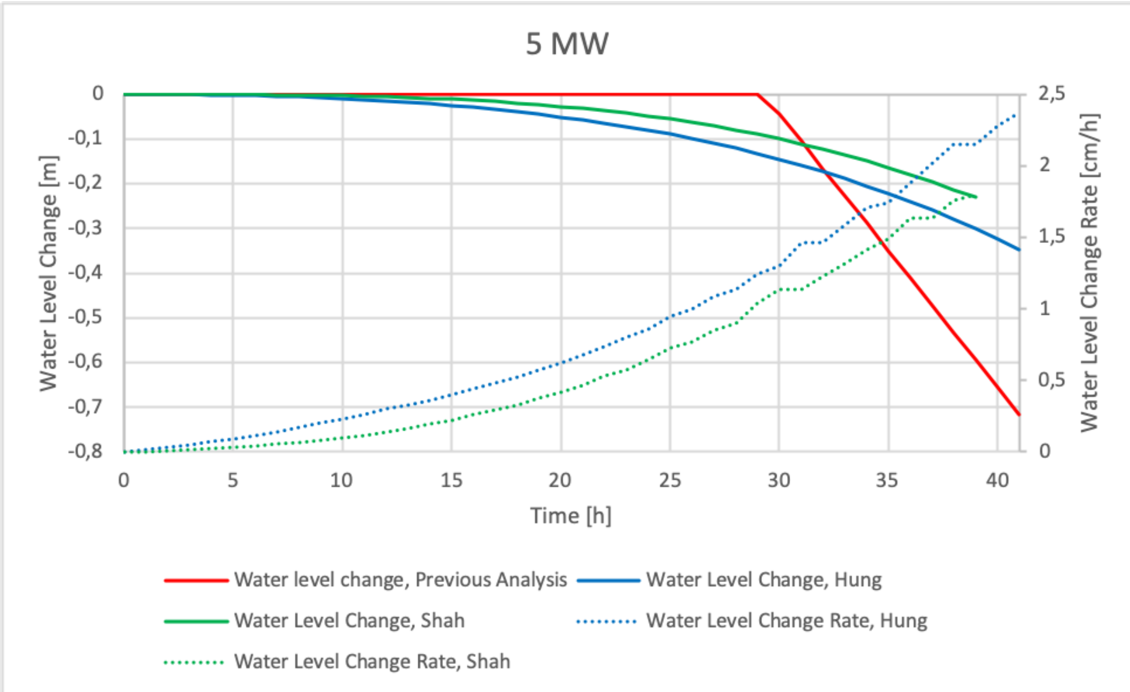

Figure 4.13: Water levels for previous and new analysis, 5MW

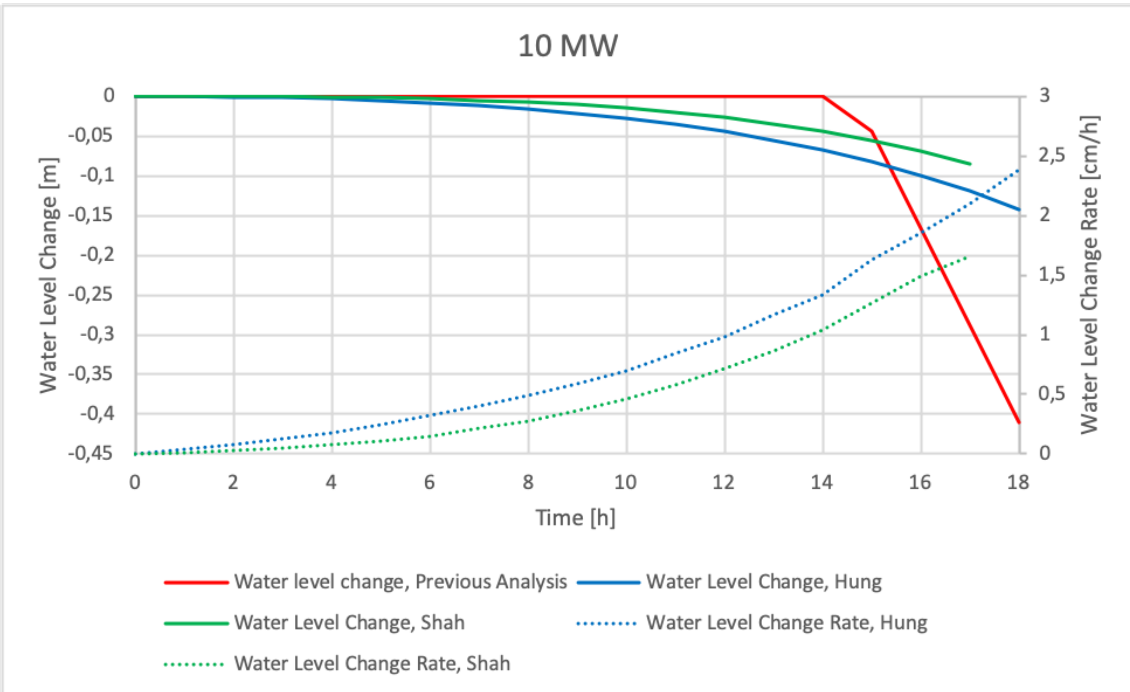

Figure 4.14: Water levels for previous and new analysis, 10MW. Note: The non linear behaviour of the red curve is only due to the data being plotted in full hour steps.

4.3 Sensitivity Studies

Results from sensitivity studies can be found in subsection 4.3.1, Relative Humidity and subsection 4.3.2, Water level. The sensitivity studies that have been carried out are different relative humidities and a lowered water level. The sensitivity studies have been done with a residual heat of 1.5MW due to it being close to the highest residual heat in the SFP during normal operation, and is one of the higher residual heats where the evaporation has great influence on the time course.

4.3.1 Relative Humidity

As shown in Figure 4.15, the relative humidity has no significant impact on the result. For conservatism, the relative humidity in the model has been set to 100%. This is implemented in Comsol's heat transfer module and is applied on all results.

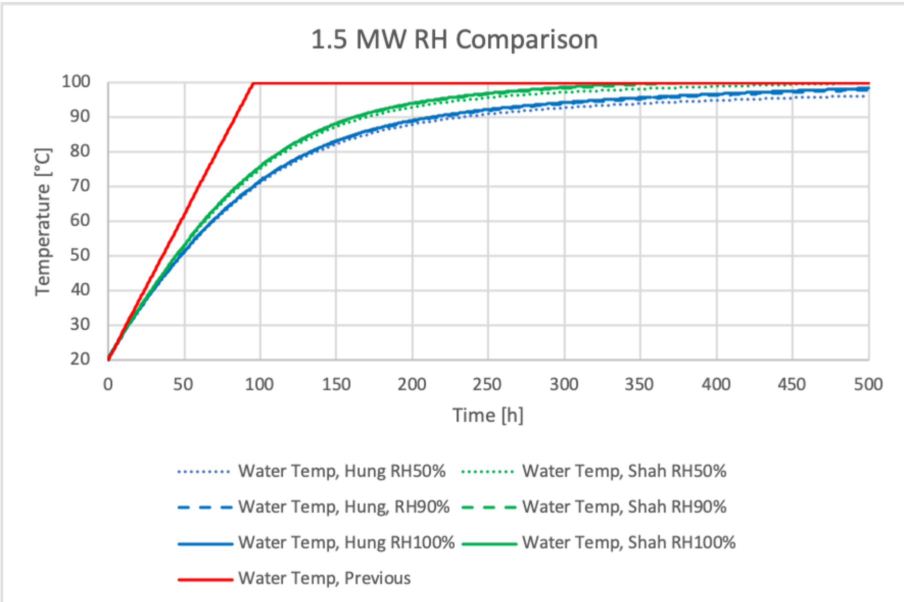

Figure 4.15: Comparisons between analysis' using different relative humidities

4.3.2 Water level

As previously mentioned, the difference in water level has not been modelled geometrically, but has subsequently been calculated, see subsection 3.2.5, Water Level Change. Because of this, a sensitivity study has been made where the water level is reduced by 2 meters. The result shows that the water level has a greater impact at lower temperatures, but that at higher temperatures when the evaporation is a significant part of the heat losses from the water, the temperature curves approach each other, see Figure 4.16, Comparisons between analysis' with full water level and 2m lower water level. (Hung model).

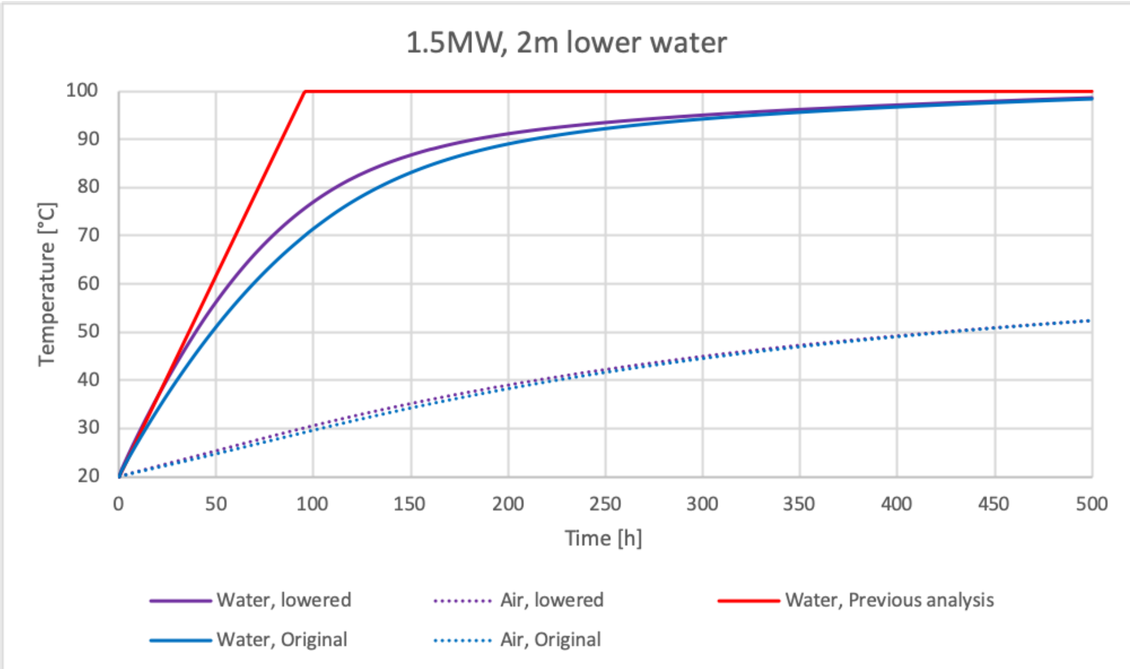

Figure 4.16: Comparisons between analysis' with full water level and 2m lower water level. (Hung model)

Worth to mention is that the water level change reaches 2m after about 250 hours at 1.5MW, meaning that if the water level change was modelled geometrically during the simulation, the temperature would be closer to the one with the original water level.

4.4 Validation of Evaporation Models

To validate the evaporation models, an analysis from the SFP at Fukushima-Daiichi unit 4 has been used as a reference.[11] The analysis has assumed a constant air temperature of 20°C with 50% relative humidity, as the building was not intact due to hydrogen explosion. Analyzes or measurement data without a constant air temperature have unfortunately not been found. Figure 4.17, Comparison with Fukushima-Daiichi SFP4 equilibrium temperature contain a figure where the same condition is used, which gave a equilibrium temperature of slightly above 86°C for Hung and slightly above 95°C for Shah. In the Fukushima-Daiichi SFP4 report, a equilibrium temperature of about 84°C was obtained. Values of equilibrium temperatures in Fukushima-Daiichi SFP4 have been obtained with the same model as Hung and have a water surface area that is about 10% less, meaning that the heat losses from evaporation should be smaller.

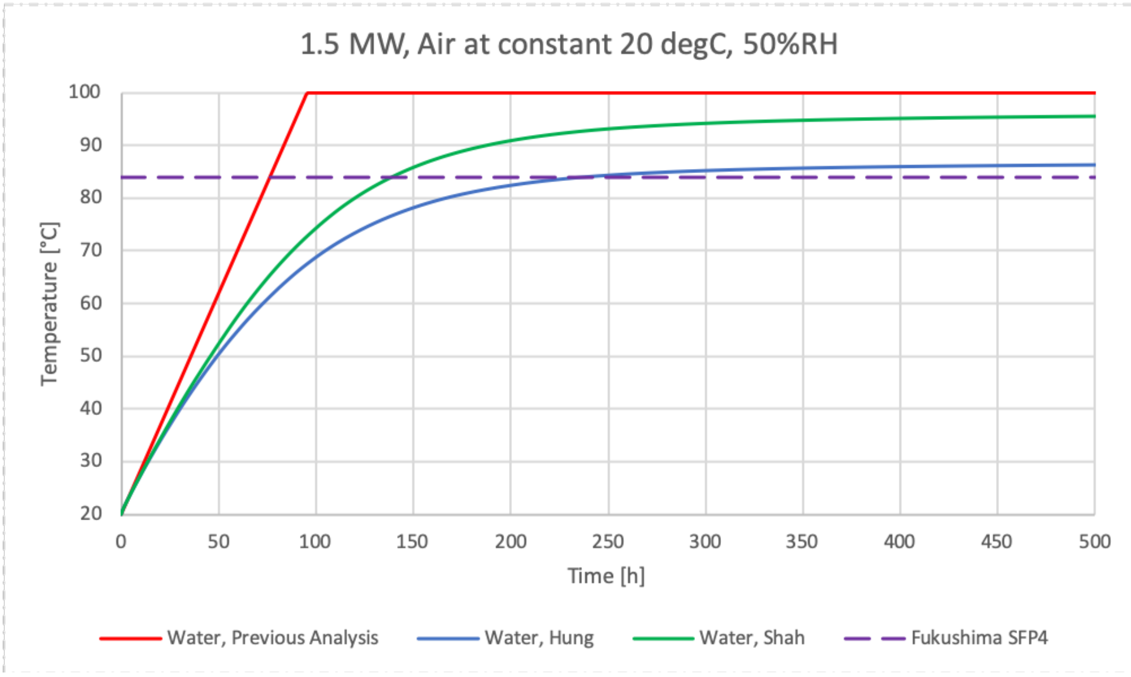

Figure 4.17: Comparison with Fukushima-Daiichi SFP4 equilibrium temperature

5
Conclusion

The results of the analysis done in this thesis have shown that the previous analysis is very conservative in its estimations of the time-dependence of the water temperature in the SFP, especially during normal operation when the residual heat in the SFP is relatively low. It has also been shown that the assumption of no evaporation before the pool reaches boiling is non-conservative in regards to the assessment of the water level at early times after loss of cooling. The times to actual uncovering of the fuel is however estimated in a conservative manner in the previous analysis.

These new results can be used when doing priorities in catastrophic events that causes a loss of cooling in the SFP. If an action in regards to the cooling of the SFP is highly prioritized due to the rising temperatures it might get a lower priority in favor of more important actions. Another important conclusion from these new results is that the water level can be lowered significantly without the temperatures in the water being close to boiling. An operator relying only on the previous analysis noting a lowering water level with temperatures well below boiling might draw the conclusion that the SFP is leaking. If this erroneous conclusion is drawn during a nuclear disaster, very valuable time will be spent on efforts in regards to fixing a leakage that does not exist.

A part of this work was to evaluate the usability of Comsol Multiphysics for these types of analyzes. Comsol has proven to yield good results with a very small amount of computing time in comparison with traditional CFD software. The customizability of the physics and multiphysics modules makes it suitable for a lot of different types of problems and its relatively short computational times might be helpful where one might hesitate to do a CFD analysis due to the time consuming process. However, the failure to get the moisture transport module to work for this problem has been a disappointment, and has meant that empirical models for evaporation have been used. Evaporation being the main difference between this and the previous analysis, along with the lack of empirical models or data for condensation, calls for further studies to be made in order to accurately assess the behaviour of the moisture transport in the fuel building.

Bibliography

[1] Batchelor, G. K. (1967) *An Introduction to Fluid Dynamics. Cambridge University Press.*

[2] Howard, H. (2012) *Fluid Mechanics (Fifth Edition) Chapter 10-Computational Fluid Dynamics.*

[3] Falkovich, G. (2011) *Fluid Mechanics*

[4] Çengel, Yunus A. (2002) *Heat and Mass Transfer (Second ed.).*McGraw-Hill. Chapter 9.

[5] Ekroth, I. and Granryd, E. (2006) *Tillämpad termodynamik.* Lund: Studentlitteratur.

[6] Böckh, P. and Wetzel, T. (2012) *Heat Transfer [electronic resource].* Alemania: Springer Healthcare Ltd.

[7] T.Hung. (2011) *The development of a three-dimensional transient CFD model for predicting cooling ability of spent fuel pools.*

[8] T. Fujii, H. Imura. (1972) *Natural convection heat transfer from a plate with arbitrary inclination*, Int. J. Heat Mass Transf. 15.

[9] R.J. Goldstein, E.M. Sparrow, D.C. Jones. (1973) *Natural convection mass transfer adjacent to horizontal plates*, Int. J. Heat Mass Transf, 1025.

[10] M. Shah. (2018) *Improved model for calculation of evaporation from water pools*, Science and Technology for the Built Environment.

[11] D.Wang. (2012) *Study of Dukushima Daiichi Nuclear Power Station Unit 4 Spent-Fuel Pool*, Oak Ridge National Laboratory.

[12] https://www.comsol.com/heat-transfer-module, Read:04-2019